

Physical Properties of Poly(β -hydroxy butyrate). III. Folding of Helical Segments in 2,2,2-Trifluoroethanol

J. Cornibert,^{1a} R. H. Marchessault,^{1b} H. Benoit, and G. Weill

Centre de Recherche pour les Macromolécules, Strasbourg, France. Received April 8, 1970

ABSTRACT: A series of samples of poly(β -hydroxy butyrate) in solution in 2,2,2-trifluoroethanol have been studied by means of light scattering. From asymptotic behavior of the angular scattering, results can be interpreted in terms of a relatively rigid rodlike particle with a linear density larger than that of the crystallographic helix. This implies a folding of helical segments leading to a model which is self-consistent with the hydrodynamic data in the same solvent.

Poly(β -hydroxy butyrate) (PHB) is a crystalline stereoregular naturally occurring polyester. In the crystalline state its conformation is that of a right-handed helix with a twofold axis along the chain corresponding to two residues per turn,² the advance per turn (pitch) being 5.96 Å. In the native state, the same helix appears to be present but a definite difference in morphology seems to occur compared to solvent-cast films. The latter are predominantly spherulitic^{3a} while a fibrous texture dominates in the native granules.^{3b}

In solution, PHB shows an abrupt change in optical rotation characteristic of a cooperative transition, when solvent composition is varied at constant temperature or temperature is varied for a given solvent composition.⁴ This phenomenon has been an important diagnostic tool for establishment of the "helix-coil" transition phenomenon in polypeptide systems. In the present case the interpretation is complicated by the fact that hydrodynamic properties such as intrinsic viscosity and sedimentation constant measured in chloroform do not follow the expected dependence on molecular weight for samples with rigid rod behavior in solution. An interrupted helix model was assumed by Okamura⁵ in order to explain the observed relation between molecular weight and intrinsic viscosity in chloroform. The junction points were envisaged to have a range of flexibilities due to dipolar interaction between helical segments of the same chain so that a dynamic ellipsoidal structure was proposed.

Light-scattering measurements in 2,2,2-trifluoroethanol (TFE) have allowed a better definition of this model, and the modified model discussed below explains both the viscosity and light-scattering data in this solvent.

Light-Scattering Measurements in TFE. Figure 1 is a

Zimm plot of PHB in TFE. Extrapolations are carried out to $\theta = 0$ and $c = 0$ giving

$$\begin{aligned} \left(\frac{Kc}{\Delta R} \right)_{\theta=0} &= \frac{1}{\bar{M}_w} + 2Bc \\ \left(\frac{Kc}{\Delta R} \right)_{c=0} &= \frac{1}{\bar{M}_w} P(\theta)^{-1} \end{aligned} \quad (1)$$

where \bar{M}_w is the weight average molecular weight, B is the second virial coefficient, c is the concentration of the dissolved polymer, $P(\theta)$ is a form factor which depends on the shape of the molecule in solution, and ΔR is the Rayleigh ratio increment. For rodlike particles of length L it is convenient to use the parameter hL , where $h = (4\pi/\lambda)n_0 \sin(\theta/2)$, λ is the wavelength of the incident light under vacuum and n_0 is the refractive index of the solvent. When $hL \rightarrow 0$ the function $P(\theta)$ can be represented as a series expansion in terms of h . If we limit ourselves to the two first terms, one obtains

$$P(\theta) = 1 - \frac{h^2 \bar{R}^2}{3} \quad (2)$$

where \bar{R}^2 is the mean square radius of gyration of the particle. When $hL \rightarrow \infty$, the asymptotic behavior of $P(\theta)$ depends on the geometry of the particle. For rigid rods, Holtzer⁶ has shown that

$$\left(\frac{h\Delta R}{\pi Kc} \right)_{c=0}^{hL \rightarrow \infty} = \frac{M}{L} \left(1 - \frac{2}{\pi hL} \right) \quad (3)$$

This function extrapolates to the limit M/L , the mass per unit length, for increasing values of h . On the other hand for a chain made up of stiff rods joined by flexible points, this same limit is reached by decreasing values of the function.⁷

The samples studied were those described in the preceding paper⁴ and the same labels are used here. The solvent, TFE, was purchased from Peninsular Chemresearch and was used "as received;" for reuse it was freshly distilled on a spinning band column each time. Before each measurement, solvent and solutions were first of all filtered then centrifuged for 2 hr at 14,000 rpm. The refractive index increment, dn/dc , of PHB in TFE was measured using a Bryce-Phoenix differential refractometer at room temperature. The light-scattering

(1) (a) Chemistry Department, University of Montreal, Montreal, Quebec; (b) on leave from the State University of New York, College of Forestry, Syracuse, N. Y.; address correspondence to this author at the Chemistry Department, University of Montreal, Montreal, Quebec, Canada.

(2) K. Okamura and R. H. Marchessault in "Conformation of Biopolymers," G. N. Ramachandran, Ed., Vol. 2, Academic Press, New York, N. Y., 1967, p 709.

(3) (a) R. Alper, D. G. Lundgren, R. H. Marchessault, and W. A. Côté, *Biopolymers*, **1**, 545 (1963); (b) D. Ellar, D. G. Lundgren, K. Okamura, and R. H. Marchessault, *J. Mol. Biol.*, **35**, 489 (1968).

(4) R. H. Marchessault, K. Okamura and C. J. Su., *Macromolecules*, **3**, 735 (1970).

(5) K. Okamura, Ph.D. Thesis, State University of New York, College of Forestry, Syracuse, N. Y., 1967.

(6) A. Holtzer, *J. Polym. Sci.*, **17**, 432 (1955).

(7) V. Luzzati and H. Benoit, *Acta Crystallogr.*, **14**, 297 (1961).

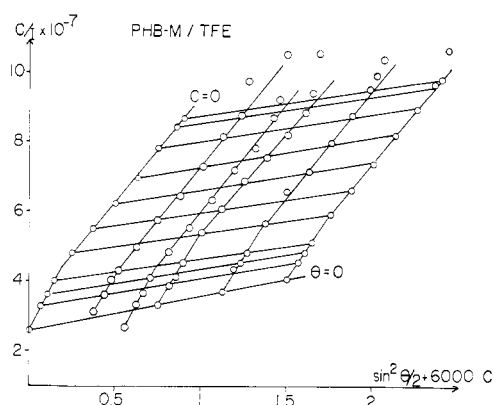


Figure 1. Zimm plot of sample M of $\bar{M}_w = 1.01 \times 10^6$ in trifluoroethanol.

tering measurements were made on a Sofica light-scattering photometer designed by Wippler and Scheibling.⁸

In Table I are gathered the \bar{M}_w and the \bar{R}^2 values determined from the Zimm plots for different samples of PHB. Also included are the number average molecular weights \bar{M}_n determined in the previous study.

Figure 2 demonstrates the asymptotic behavior of the different PHB samples which were studied. For the three highest molecular weights a typical rodlike behavior is observed since at high angle the plotted function shows asymptotic behavior. According to eq 3 the asymptote provides a measure of M/L . The fact that the asymptote is different for each curve indicates a variation in linear density.

If we assume the rigid rod model, one can calculate the average length, \bar{L} , from the radius of gyration and the relation

$$\bar{L}^2 = 12\bar{R}^2 \quad (4)$$

and from this value, one obtains \bar{M}_w/\bar{L} which should be equal to $(M/L)_{\text{asympt}}$ obtained from the asymptotic behavior assuming the system is monodispersed. Since the average based on L is of higher order than that based on M , the effect of polydispersity should lead to a somewhat lower value for the former ratio. However, there is a remarkable agreement between the two ratios as may be judged from the data in Table I.

TABLE I
 \bar{M}_w AND MOLECULAR PARAMETERS BY LIGHT SCATTERING AT ROOM TEMPERATURE ($\approx 22^\circ$) FOR PHB SAMPLES IN TFE

Samples	M	E	K	J
\bar{M}_w	1.01×10^6	8.4×10^5	3.8×10^5	1.35×10^5
\bar{M}_w (sed) ^a		7.8×10^5	3.7×10^5	
\bar{M}_n		1.27×10^5	8.5×10^4	
$\bar{R}^2, \text{\AA}^2$	1.25×10^6	0.94×10^6	0.42×10^6	0.23×10^6
$\bar{L}, \text{\AA}$	3900	3400	2250	1700
$b, \text{\AA}$	13.0	12.7	10.5	7.2
$p = \bar{L}/2b$	149	132	107	115
$(M/L)_{\text{asympt}}$	280	260	180	
$\bar{M}_w/\bar{L}, \text{g/\AA}$	260	250	170	81

^a Sedimentation, osmometry data in CHCl_3 taken from the previous paper.⁴

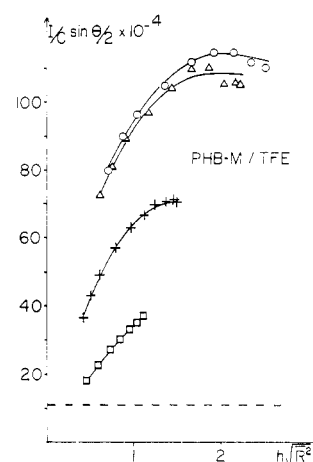


Figure 2. Asymptotic scattering behavior of samples M (O), E (Δ), K (+), and J (\square) in trifluoroethanol. The plot shows the reduced scattered intensity, I/C , plotted against the parameter $h\sqrt{R^2}$ and the dotted line corresponds to the asymptotic value for the crystallographic helix.

The most noteworthy fact concerning the data in Table I is that the values for the mass per unit length, linear density, derived from solution studies are much greater than the value of 28.9 g/\AA , calculated from the crystallographic helix² proposed for PHB. The latter value is shown as a dotted line in Figure 2.

In order to explain these results, two hypotheses come to mind: that of the "superhelix" and the "folded chain" model. The former is to be rejected on the basis of the observed variation of M/L with M ; superhelices such as DNA always maintain a constant value of this ratio. Only the chain-folding hypotheses can readily take into account the regular increase of linear density with molecular weight which would imply an increase in the number of folds as the chain length gets longer, the driving force being a delicate balance between surface/volume and fold energy. It is to be noted that from the slope of the Zimm plot TFE is classed as a "good" solvent.

In terms of the chain-folding hypothesis, it is interesting to consider the influence of temperature on the linear density. We have studied the sample whose weight average molecular weight corresponds to 1.01×10^6 between 14.5 and 68° . The decrease in the value of dn/dc and the increase in the value of Rayleigh constant R_b for benzene⁹ as the temperature increases were taken into account

$$\left(\frac{dn}{dc}\right)_T = 0.160 - 0.028T \quad (5)$$

$$(R_b)_T = 16.3 \times 10^{-6} [1 + 0.368 \times 10^{-2}(T - 25)]$$

where the temperature is in degrees centigrade. The solutions and the light-scattering bath were kept at constant temperature by means of a circulating thermostat. As temperature increased, the following observations were made: the weight average molecular weight does not change; \bar{L} of the rod, calculated from the

(8) G. Wippler and G. Scheibling, *J. Chim. Phys.*, **51**, 201 (1954).

(9) J. Ehl, Mémoire D. E. S., Université de Strasbourg, France, 1963.

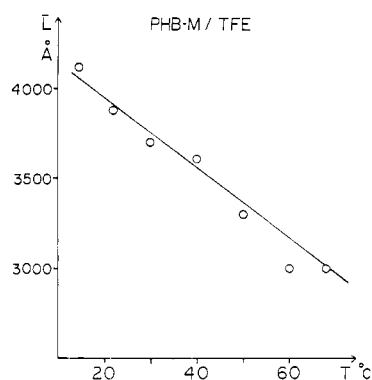


Figure 3. Plot of the average rod length, \bar{L} , vs. temperature, T , for sample M of $\bar{M}_w = 1.01 \times 10^6$ in trifluoroethanol.

observed value for the radius of gyration, decreases linearly (Figure 3) and as a result M/L increases.

In terms of the chain-folding hypothesis the number of folded segments increases with temperature. It is worth noting that this is just the opposite to what is found when solid polymers are annealed in an inert atmosphere.¹⁰

By linear regression analysis it was found that the two straight lines corresponding to the variation of \bar{M}_w/\bar{L} and $(M/L)_{\text{asympt}}$ as a function of temperature are parallel and can even be taken as identical (Figure 4).

Given the value of \bar{L} one can calculate the diameter $2b$ and the axial ratio p of the equivalent ellipsoid whose volume is given by

$$\frac{\bar{M}_w}{N_A \rho} = \frac{4}{3} \pi \frac{\bar{L}}{2} b^2 \quad (6)$$

where N_A is Avogadro's number and we have taken the dry density¹ of PHB as the value for ρ of the compact rod in solution. The results are shown in Table I. In terms of the chain-folding hypothesis, the increase in b as a function of the weight average molecular weight is not surprising. It implies that the equivalent ellipsoid increases in diameter faster than in length, which is in keeping with the hydrodynamic data. From the latter alone, however, one would not have arrived at the conclusion that a compact asymmetric particle was involved.

Intrinsic Viscosities in TFE. Intrinsic viscosities at 30° for different samples of PHB in trifluoroethanol were measured in a Ubbelohde-type viscometer which has a shear rate of approximately 500 sec⁻¹.⁴ The flow time of the solvent was sufficiently great for neglect of the kinetic energy correction.

Figure 5 shows the variations of $\log [\eta]$ as a function of $\log \bar{M}_w$ for PHB in TFE. In terms of the Mark-Houwink equation, the following relation is obtained

$$[\eta] = 2.51 \times 10^{-4} \bar{M}_w^{0.74} \quad (7)$$

A necessary but not sufficient condition for the molecule to correspond to a rigid ellipsoid of constant diameter is that the exponent, a , be greater than unity. For flexible molecules, the exponent is found to be between 0.5 and 0.8.¹¹

(10) A. Keller, *Polymer*, **3**, 393 (1962).

(11) G. Spach, L. Freund, M. Daune, and H. Benoit, *J. Mol. Biol.*, **7**, 468 (1963).

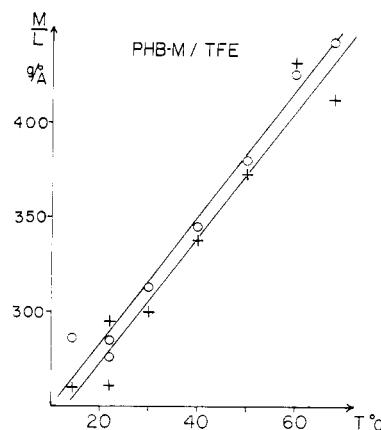


Figure 4. Plots of linear densities $(M/L)_{\text{asympt}}$ (O) and \bar{M}_w/L (+), vs. temperature, T , for sample M in trifluoroethanol.

Another criterion of rigidity was proposed by Daune¹² and is obtained by plotting $M^2/[\eta]$ as a function of $\log M$. Thus for ellipsoids of revolution, we have the following relationship which is valid over a large range of rod lengths

$$\frac{M^2}{[\eta]} = \frac{45}{2\pi N_A} (M/L)^3 \log M + B \quad (8)$$

where B is a constant. In the case of rigid particles whose length is proportional to the mass and whose diameter is constant, the points should fall on a straight line whose slope is proportional to the mass per unit length. The flexibility of the rod shows itself by an upward curvature of the type seen in Figure 6, where $\bar{M}_w^2/[\eta]$ is plotted as a function of $\log \bar{M}_w$.

In the absence of other information, one would conclude from the foregoing data that the molecule is flexible. However, knowing that the mass per unit length and the diameter are varying with the molecular weight, as shown by the light-scattering measurements, these results must be interpreted otherwise. In fact this is a good example of how one can be led astray when one uses the hydrodynamic approach alone. Qualitatively the axial ratio, p , varies as some fractional exponent of the mass, and this explains why one has relatively small values of a in spite of the fact that we are dealing with a rigid particle as shown by light scattering.

Assuming the molecular particles correspond to

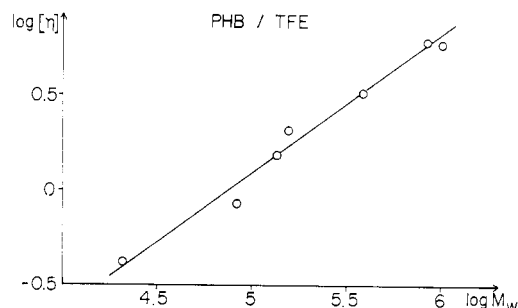


Figure 5. Double logarithmic plot of $[\eta]$ in trifluoroethanol vs. \bar{M}_w for data in Table II.

(12) M. Daune, L. Freund, and G. Spach, *J. Chim. Phys.*, **59**, 485 (1962).

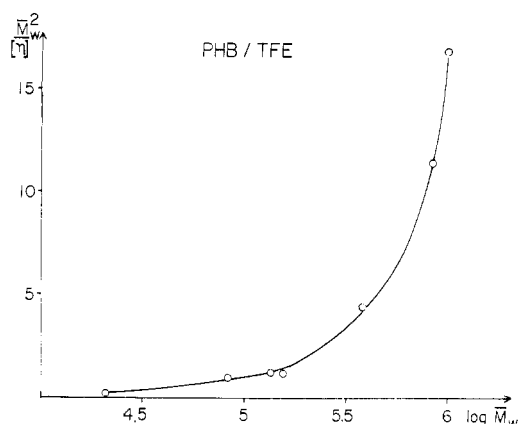


Figure 6. Daune's criterion of rigidity: plot of $\bar{M}_w^2 [\eta]_{\text{TFE}}$ vs. $\log \bar{M}_w$.

prolate ellipsoids of revolution, that is, prolate ellipsoids which are rigid, very long, and compact, the intrinsic viscosity can be written in the form

$$[\eta] = v_{sp} \Lambda(p) \quad (9)$$

where p and v_{sp} are, respectively, the axial ratio of the ellipsoid, $p = a/b$, and the specific volume of the dissolved substance. The function $\Lambda(p)$ is a form factor which is obtained from tables compiled by Simha.¹³

In Table II we have gathered together the parameter for the particles which are calculated by combining relations 6 and 9 using for v_{sp} the dry specific volume² of PHB, that is, 0.812 cm³/g. There is relatively good agreement between these parameters and those which have been calculated from the light-scattering results as shown in Figure 7.

Effect of Shear Rate and Temperature on Intrinsic Viscosity Data. We have seen from the light-scattering data that the particle length decreases with increasing temperature. In Figure 7 we have compared light-scattering results which were performed at room temperature, that is, 22°, and intrinsic viscosity data recorded at 30° which, in view of the above mentioned effect of temperature on the length, are not quite valid. This explains, in part, why the values of L_{visc} are always

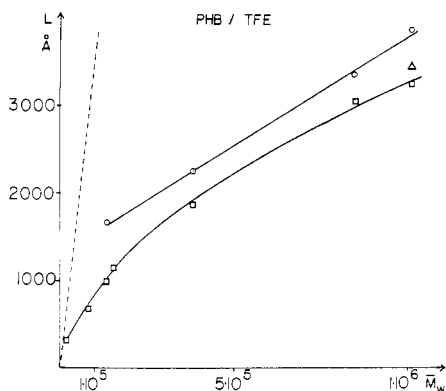


Figure 7. Plot of the rod length \bar{L} (O), L_{visc} (□), and L from the intrinsic viscosity at low rate of shear (Δ) vs. \bar{M}_w . The dotted line corresponds to the length of the crystallographic helix for PHB in trifluoroethanol.

(13) R. Simha, *J. Phys. Chem.*, **44**, 25 (1940).

TABLE II
[η] AND MOLECULAR PARAMETERS IN TFE
AT 30° FOR PHB SAMPLE

Samples	\bar{M}_w	$[\eta]$, dl/g ^a	p_{visc}	b_{visc} , Å	$L_{\text{visc}} = 2a$, Å
M	1.01×10^6	6.08	115	14.2	3300
E	8.4×10^5	6.20	115	13.3	3100
K	3.8×10^5	3.31	81	11.5	1870
B ^a	1.56×10^5	2.11	63	9.3	1170
J	1.35×10^5	1.55	53	9.4	990
C ^a	8.35×10^4	0.85	37	9.0	670
F ^a	2.11×10^4	0.42	24	6.5	320

^a Data taken from the previous paper.⁴

TABLE III
COMPARISON OF MOLECULAR PARAMETERS DERIVED FROM
LIGHT SCATTERING AND "LOW SHEAR" VISCOSITY
DATA FOR SAMPLE M

Parameters	p	$L = 2a$, Å	b , Å	M/L , g/Å
$[\eta]_{G \rightarrow 0} = 6.9$ dl/g	123	3400	13.9	290
Light scattering	133	3700	13.3	300

somewhat less than \bar{L} (Figure 7). The difference may also be due to a significant non-Newtonian viscosity effect¹⁴ which in the case of rod will be all the greater the longer the particle or axial ratio. In order to evaluate this factor, we have measured the intrinsic viscosity of sample M at 30° using a Couette-type viscometer which allows measurements at low rates of shear (approximately 4–5 sec⁻¹). The result and the corresponding parameters are shown in Table III along with the parameters calculated from light scattering at the same temperature. Considering the precision of these types of measurements, one must consider that the agreement is rather good.

Light-scattering results have shown that the length of the rod decreases with increasing temperature and the intrinsic viscosity would of course be expected to show

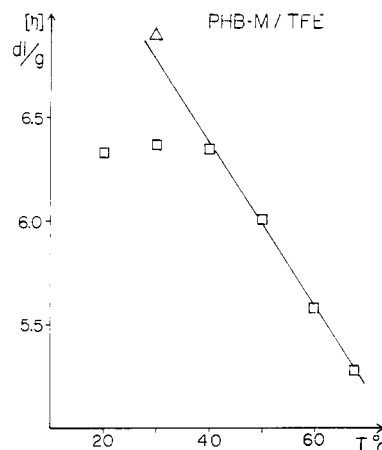


Figure 8. Plot of intrinsic viscosity $[\eta]$ vs. temperature, T , for sample M of $\bar{M}_w = 1.01 \times 10^6$ in trifluoroethanol; $[\eta]$ with a Ubbelohde viscometer (□) and $[\eta]$ at low rate of shear (Δ).

(14) J. T. Yang, *J. Amer. Chem. Soc.*, **80**, 1783 (1958).

the same behavior. Again for sample M we have measured intrinsic viscosity for the temperature range between 20.0 and 67.5° using a dilution viscometer of the Ubbelohde type,¹⁵ with no correction applied for rate of shear effects. The results are shown in Figure 8 and while one does find a definite decrease in viscosity with temperature, as would be predicted from the light-scattering data, there is a disturbing horizontal tangent at the lower temperatures. It is believed that this is due to the important contribution of non-Newtonian viscosity at these lower temperatures which correspond to axial ratios where one would expect a significant effect of this kind. In fact, the value of intrinsic viscosity obtained in the low shear viscometer at 30° does indeed fall on the extrapolation of the straight line in Figure 8.

Conclusions

We have seen that the results can be interpreted in terms of the chain-folding hypothesis, that is, the chain folding of helical segments on themselves in order to form a compact rigid particle. If one supposes that these helical segments correspond to the crystallographic helix whose mass per unit length is 28.9 g/Å, then for a given molecular weight it is possible to calculate the length L_{cryst} of the helix in the completely extended state. From this value one can then calculate the ratio $n = L_{\text{cryst}}/\bar{L}$ or $L_{\text{cryst}}/L_{\text{visc}}$ which implies $(n - 1)$ folds in a rod whose total length is \bar{L} or L_{visc} .

Since we know the diameter of the crystallographic helix, it is therefore possible, on the basis of this model, to calculate the diameter $2b$ of the rod. Values for this diameter corresponding to different degrees of chain folding are shown in Table IV using as helical diameter for the crystallographic helix 6.6 Å which is one-half of the b axis in the unit cell proposed by Okamura and Marchessault.² These data have been plotted as a function of n in Figure 9. The values thus calculated can be favorably compared to the corresponding variations in diameter $2b$ which were deduced from the light-scattering and viscosity results.

Although these are obvious inaccuracies and assump-

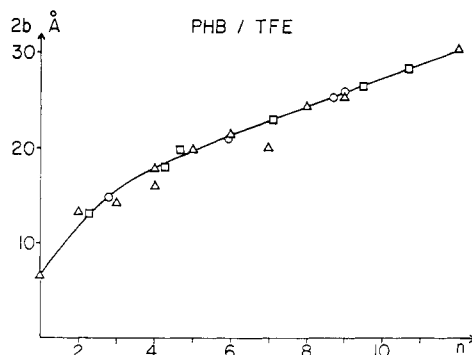


Figure 9. Plot of the diameter of the rod $2b$ vs. $n = L_{\text{cryst}}/\bar{L}$ or $L_{\text{cryst}}/L_{\text{visc}}$ for PHB in trifluoroethanol: (Δ), $2b$ calculated for different degrees of chain folding; (O), $2b$ deduced from the light-scattering results; (\square), $2b$ deduced from the viscosity results.

tions involved in the foregoing analysis, there is in general a good self-consistency and one must conclude that the chain-folding hypothesis implying a relatively compact rigid particle seems to account for the hydrodynamic and light-scattering data recorded for solutions of PHB in trifluoroethanol. Admittedly, this interpretation rests mainly on the angular dependence of the light-scattering results. The molecular weight dependence of the radius of gyration and viscosity would more usually be related to a flexible molecule. However, there are several features to the PHB helix conformation as well as the helix-coil behavior mentioned in the previous paper which make the chain-folding hypothesis still more plausible.

Since PHB possesses a significant dipole moment along its length due to the molecular sense of the polyester and the strong polarity of the carbonyl group, chain folding can be stabilized by an attractive interaction between these helical segment dipoles. This attraction may be quite sufficient to overcome the entropic factor which would encourage a less ordered state in solution and the strain factor which is operative at the fold surfaces. Although this appears to be the first time that the chain-folding model has been invoked in order to explain light scattering and hydrodynamic data of the type described above, Poland and Scheraga¹⁶ have already considered a similar model, in its theoretical implications, for a 20 residue helix of poly-L-alanine and have come to the following conclusions: chain folding is quite probable; there is no unique folded structure at a given temperature but a variety of folded species are possible corresponding to two folds, three folds, four folds, etc., and there is a most probable structure; the number of folds increases with temperature until one approaches the "helix-coil" transition zone.

A more detailed study of chain folding in different solvents and for a wider range of temperature and molecular weight is called for in order to provide further evidence on this type of secondary structure.

TABLE IV

n	MODELS	$2b$ Å	n	MODELS	$2b$ Å
2		13.2	6		21.4
3		14.2	7		19.8
		18.0	8		24.6
4		16.0	9		25.3
5		19.8	12		30.4

(15) P. Gramain and R. Libeyre, *J. Appl. Polym. Sci.*, **14**, 383 (1970).

(16) D. Poland and H. A. Scheraga, "Poly- α -Amino Acids," Vol. 1, G. D. Fasman, Ed., Marcel Dekker, New York, N. Y., 1967, p 478.

It is to be noted, however, that chain folding is a widely accepted mechanism for the crystallization of synthetic high polymers¹⁰ as well as many natural linear polymers. For these systems it is admitted that the extended chain form is unquestionably the most stable, since a fold usually represents molecular distortion and strain.

However, folding is tolerated since kinetic factors control the crystallization and, as a result of this, the effect of temperature is to increase the length of chain segments between folds. This is clearly the opposite to what has been observed in our case and suggests an important influence of solvent on the phenomenon.

Polymerization of Ferrocenylmethyl Acrylate and Ferrocenylmethyl Methacrylate. Characterization of Their Polymers and Their Polymeric Ferricinium Salts. Extension to Poly(ferrocenylethylene)

Charles U. Pittman, Jr.,^{1a} J. C. Lai,^{1b} D. P. Vanderpool,^{1c} Mary Good,^{1d} and Ronald Prado^{1e}

Department of Chemistry, University of Alabama, University, Alabama 35486, and Louisiana State University in New Orleans, New Orleans, Louisiana 70122.

Received June 15, 1970

ABSTRACT: Poly(ferrocenylmethyl acrylate), poly(ferrocenylmethyl methacrylate), and poly(ferrocenylethylene) have been prepared by AIBN-catalyzed, free-radical polymerization in benzene solution. Treatment of these polymers with strongly electron attracting compounds such as tetracyanoethylene, dichlorodicyanoquinone, and *o*-chloranil leads to poly(ferricinium) salts, or polymeric charge-transfer derivatives. The characterization of these polymers was carried out by kinetic studies, infrared, nuclear magnetic resonance, ultraviolet, and Mössbauer spectroscopy, as well as gel permeation chromatography and viscosity studies. Some of these studies must be carried out before treatment with the electron acceptor. Mössbauer spectroscopy was found to be an excellent analytical technique to determine the percentage of ferrocene groups converted into ferricinium units, since iron in ferrocene groups exhibits a large quadrupole splitting (~ 2.4 mm/sec), while in ferricinium groups iron has a single peak. Each molecule of electron-attracting quinone in the poly(ferricinium) salts was present as its radical anion. Polysalts were prepared in which varying percentages of the ferrocene nuclei had been oxidized to ferricinium units. The homopolymerizations were first order in [monomer], half order in [AIBN], giving polymers with $\bar{M}_n = 5\text{--}36 \times 10^3$ before addition of electron acceptors. The activation energies were determined for the first-order polymerizations.

Over the past 15 years a large variety of polymers containing ferrocene has been prepared and reviewed.² In spite of the large number of condensation polymers and unusual polymeric structures which have been prepared, references are rare to addition polymers containing ferrocene, especially free-radical-initiated addition polymers. One of the few exceptions is vinylferrocene which has been polymerized to poly(ferrocenylethylene), a tan powder melting at 280–285°, by the use of azobisisobutyronitrile (AIBN) in bulk and in solution.³ However, even poly(ferrocenyl-

ethylene), PFE, has not been extensively characterized. No previous polymerization of ferrocene-containing acrylates has been reported. One reason that reports of addition polymers of ferrocene (and other transition metal-containing organometallic compounds) are rare is that easy oxidation of the transition metal can occur instead of polymerization, with strongly oxidizing initiators. Ferrocene is readily oxidized to the stable ferricinium ion at a potential of -0.56 V.^{4a} Free radicals, formed from initiators such as benzoyl peroxide, in some cases oxidize ferrocene instead of initiating polymerization, and cations, such as the nitronium ion, oxidize ferrocene instead of attacking the cyclopentadienyl rings electrophilically. In strong acids ferrocene is protonated at iron.^{4b} Thus, in some cases normal cationic polymerization of ferrocene derivatives will be thwarted. Furthermore, initial free-radical polymerization of ferrocene derivatives can be precluded if the iron atom catalyzes either preferential decomposition of the initiator or reduces growing chain radicals.

Several factors make addition polymers of ferrocene derivatives, such as vinylferrocene and acrylates of ferrocene, of paramount interest. First, Richards⁵

(1) (a) To whom inquiries should be addressed at the University of Alabama; (b) University of Alabama, Graduate Student Research Associate (Petroleum Research Fund Fellow 1969–1970); (c) University of Alabama, Undergraduate Research Paint Research Fellow 1970; (d) Louisiana State University; (e) Louisiana State University, Graduate Student Research Associate, NSF trainee.

(2) C. U. Pittman, Jr., *J. Paint Technol.*, **39** (513), 585 (1967); H. Valot, *Double Liaison*, **130**, 775 (1966); M. Dub, "Compounds of the Transition Metals," Vol. 1, Springer-Verlag, Berlin, 1966; E. W. Neuse in "Advances in Macromolecular Chemistry," Vol. 1, M. W. Pasika, Ed., Academic Press, New York, N. Y., 1968; E. W. Neuse and H. Rosenberg, *Ferrocene Polymers*, Marcel Dekker, New York, N. Y., in press; T. P. Vishnyakova *Usp. Khim.*, **36**, 2136 (1967).

(3) F. S. Arimoto and A. C. Haven, *J. Amer. Chem. Soc.*, **77**, 6295 (1955); A. C. Haven, Jr., U. S. Patent 2,821,512 (1958); C. Y. Hua, F. Refojo, and H. G. Cassidy, *J. Polym. Sci.*, **40**, 433 (1959); M. G. Baldwin and K. E. Johnson, *ibid.*, Part A-1, **5**, 2091 (1967).

(4) (a) J. A. Page and G. Wilkinson, *J. Amer. Chem. Soc.*, **74**, 6149 (1952); (b) T. J. Curphey, J. O. Santer, M. Rosenblum, and J. H. Richards, *ibid.*, **82**, 5249 (1960).

(5) J. H. Richards, *J. Paint Technol.*, **39**, (513), 569 (1967).